

Calculation of atmospheric neutrino fluxes

M. Kawasaki and S. Mizuta

Department of Physics, Tohoku University, Sendai 980, Japan

(Received 24 September 1990)

The atmospheric neutrino fluxes at the Kamioka site are calculated semianalytically. We investigate the dependence of various physical parameters on the resultant fluxes. Both the absolute value of the fluxes and the $(\nu_e + \bar{\nu}_e)/(\nu_\mu + \bar{\nu}_\mu)$ ratio agree with those of the previous calculation. In particular, it is found that the $(\nu_e + \bar{\nu}_e)/(\nu_\mu + \bar{\nu}_\mu)$ ratio is almost independent of the method or the details of calculation.

I. INTRODUCTION

It is known that atmospheric neutrinos are produced by the decay of mesons which come from scatterings between the primary cosmic rays (mainly protons) and air nuclei:

$$\begin{aligned} \pi^\pm(K^\pm) &\rightarrow \mu^\pm + \nu_\mu(\bar{\nu}_\mu), \\ \mu^\pm &\rightarrow e^\pm + \nu_e(\bar{\nu}_e) + \bar{\nu}_\mu(\nu_\mu). \end{aligned} \quad (1)$$

Naively we expect the $(\nu_e + \bar{\nu}_e)/(\nu_\mu + \bar{\nu}_\mu)$ ratio to be 0.5. However, it was reported by the Kamiokande Collaboration¹ that the ratio of electronlike events to muonlike events is different from a theoretical expectation value in the energy range between about 0.1 and about 1 GeV. The measured value of R_{obs} , where

$$R_{\text{obs}} \equiv \frac{\text{number of electronlike events}}{\text{number of muonlike events}}, \quad (2)$$

is 1.09 ± 0.16 . On the other hand, the ratio R_{Mont} by Monte Carlo simulations based on theoretical neutrino fluxes given by Gaisser, Stanev, and Barr² is 0.61. Therefore $R_{\text{obs}}/R_{\text{Mont}}$ is 1.78 ± 0.27 , which shows a 2.9σ discrepancy. Recently new data of both R_{obs} and R_{Mont} which includes the effect of muon polarization were reported.^{3,4} According to these new data, $R_{\text{obs}}/R_{\text{Mont}}$ is 1.63 ± 0.22 and this still shows a 2.9σ discrepancy.

The observational data of other underground detectors [IMB,⁵ Fréjus,⁶ NUSEX (Ref. 7)] agree with the expectation value based on the same theoretical neutrino fluxes.^{2,4} However, they are also consistent with that of the Kamiokande Collaboration; therefore, the observational data of the Kamiokande Collaboration is not excluded or confirmed by those of other underground detectors yet.

Since this discrepancy between the observational data and the expectation value suggests that there may exist new phenomena beyond the standard model, such as neutrino oscillation,⁸ it is important to examine whether or not this discrepancy indeed exists by recalculating the neutrino fluxes at the Earth's surface.

There are already some calculations of the neutrino fluxes,^{2,4,9} but many of them estimate the fluxes by a numerical experiment with the Monte Carlo method. In a

numerical experiment, however, it is not clear what is the most essential among various physical processes which determine the atmospheric neutrino fluxes. In this paper, therefore, we calculate them in a different way from those of the previous authors. We represent them as a semi-analytical form which contains several physical parameters and finally integrate them numerically changing these parameters. By this method, we can investigate how the resultant neutrino fluxes depend on various physical processes much more easily than by a numerical experiment. Thus we can study whether or not the discrepancy of the $(\nu_e + \bar{\nu}_e)/(\nu_\mu + \bar{\nu}_\mu)$ ratio can decrease.

As seen later, it is concluded that the $(\nu_e + \bar{\nu}_e)/(\nu_\mu + \bar{\nu}_\mu)$ ratio is almost universal, which leads us to confirm the discrepancy between the observational data and the expectation value.

II. CALCULATION

A. Basic assumptions

The primary-cosmic-ray protons hit the air nuclei in the upper atmosphere and produce many pions (and kaons). Some of the pions are absorbed by air nuclei but mostly decay into muons and muon neutrinos. The produced muons lose their energy by ionizing the air atoms and most of them decay into electrons (positron) and electron neutrinos. We express the atmospheric neutrino fluxes as semianalytical form. For this end we make several assumptions on the various physical processes and the primary-cosmic-ray spectrum.

1. Primary protons

We assume a power-law momentum spectrum for the primary protons in the high-energy region ($\propto p_p^{-\alpha}$; $\alpha=2.67$). The power index α is determined from the observational data.¹⁰ However, the observed spectrum¹⁰ bends below about 3 GeV, because the solar wind blows out low-momentum protons. Furthermore, the geomagnetic field prevents low-momentum protons from reaching the Earth's atmosphere. The cutoff momentum by the Earth's geomagnetic field is approximately represented by Störmer's formula:¹¹

$$p_c = \frac{59.4 \cos^4 \lambda}{r^2 [1 + (1 - \cos^3 \lambda \sin \theta \sin \varphi)^{1/2}]^2} \text{GeV}, \quad (3)$$

where λ is the magnetic latitude, θ the zenith angle, φ the azimuthal angle measured clockwise from magnetic North, and r the distance from the dipole center (in Earth-radius units). Hence the actual cutoff momentum is the higher momentum between the cutoff momentum by the solar wind and that by the geomagnetic field.

Although the primary protons with momentum below the cutoff cannot reach the Earth's atmosphere, such low-momentum protons are produced secondarily by the scatterings between the primary protons and air nuclei. Therefore, in order to take the effects of these secondary protons into account, we assume the flat spectrum of the primary protons below the cutoff momentum. This spectrum corresponds to the case where the effect of the secondary protons is maximally taken into account. We also calculate the neutrino fluxes by neglecting the primary protons with a momentum smaller than the cutoff, in order to investigate the effect of secondary protons upon the resultant neutrino fluxes.

Note that, in the calculation of Gaisser and co-workers,^{2,4} Störmer's formula is averaged over the azimuthal angle φ and they use the averaged cutoff momentum over φ , but it is not in our case.

2. One-dimensional approximation

We take the one-dimensional approximation; i.e., we assume that the direction of the neutrinos is the same as that of the primary protons. Some low-momentum muons lose almost all of their kinetic energy and stop before their decay. As a result the emitted neutrinos are generated nearly isotropic; hence, about half of them escape without reaching the Earth's surface. Therefore the neutrino flux of the one-dimensional calculation might be about two times larger than that of the three-dimensional calculation at the low-momentum region. It is shown by Lee and Bludman,¹² however, for neutrinos with an energy greater than 200 MeV, that the result of the one-dimensional calculation is in good agreement with that of the three-dimensional one. Thus we can safely take the one-dimensional approximation for the atmospheric neutrinos which can be detected in the deep-underground detector.

3. Atmospheric density

The atmospheric density profile is assumed to be represented by a single exponential:

$$\rho(h) = \rho_0 \exp \left[-\frac{h}{h_0} \right], \quad (4)$$

where h is the altitude measured vertically from the Earth's surface and h_0 is the scale parameter of the upper atmosphere ($h_0 = 6.42$ km). We determine ρ_0 so that the column density calculated by this formula corresponds to the measured one and we get $\rho_0 = 1.61$ kg/m³. It is reasonable to determine ρ_0 in this way, because the energy loss of the muons depends only on the column density.

An actual atmospheric density on the Earth's surface is a little smaller than ρ_0 , but this difference has only a negligible effect on the neutrino fluxes.

4. Pion production

We assume that the pion-production momentum spectrum is given by

$$\frac{d\Gamma_\pi(x)}{dx} = \frac{(1-x)^3}{x^p}, \quad (5)$$

where x is the fractional momentum of a pion in the laboratory system ($x \equiv$ pion momentum/proton momentum). Here the normalization factor is neglected and it is discussed later. Since the value of p in the pion-production momentum spectrum is not well known (usually $p = 1$ is used), we calculate the muon fluxes and neutrino fluxes at the Earth's surface with different values of p , and investigate the dependence of the resultant muon and neutrino fluxes on p .

5. Effect of K meson

We neglect K mesons which are produced by scatterings between the primary protons and air nuclei. Experimentally the K/π ratio in a hadron interaction is known to be about 10% averaged over $+$, $-$ charges.¹³ Therefore, the effect of K mesons upon the resultant neutrino fluxes is small. In fact, we can estimate the effect of K mesons upon the resultant $(\nu_e + \bar{\nu}_e)/(\nu_\mu + \bar{\nu}_\mu)$ ratio by calculating neutrino fluxes for the channel, $K^\pm \rightarrow \mu^\pm + \nu_\mu(\bar{\nu}_\mu)$, $\mu^\pm \rightarrow e^\pm + \nu_e(\bar{\nu}_e) + \bar{\nu}_\mu(\nu_\mu)$, and it is found that K mesons could reduce the $(\nu_e + \bar{\nu}_e)/(\nu_\mu + \bar{\nu}_\mu)$ ratio by at most 4% which would rather enlarge the discrepancy between R_{obs} and R_{Mont} .

6. Normalization factor

Since, in this calculation, the effects of the secondary protons and/or the secondary pions are taken into account only partially, the overall normalization factor of neutrino fluxes is not determined theoretically. Therefore the normalization factor is fixed by comparing the calculated muon flux at the Earth's surface with the observational one.¹⁴ Note that the $(\nu_e + \bar{\nu}_e)/(\nu_\mu + \bar{\nu}_\mu)$ ratio is independent of this normalization factor.

7. Muon polarization

We take into account the polarization of the muon from a pion decay.¹⁵ It is well known that μ^- (μ^+) from π^- (π^+) decay is completely polarized to helicity $+$ ($-$) in the pion rest frame. This muon polarization remains about 30% in the laboratory system, and it increases the $(\nu_e + \bar{\nu}_e)/(\nu_\mu + \bar{\nu}_\mu)$ ratio in the high-energy region, because $\bar{\nu}_e$ (ν_e) from the decay of μ^- (μ^+) which is polarized to helicity $+$ ($-$) has a higher energy compared with the unpolarized case.

In the muon rest frame, the decay distributions of $\bar{\nu}_e$ and ν_μ from the decay $\mu^- \rightarrow e^- + \bar{\nu}_e + \nu_\mu$ are

$$\begin{aligned} \bar{\nu}_e: d\Gamma &= \frac{m_\mu^5 G^5}{32\pi^3} \bar{x}^2 (1-\bar{x})(1+\cos\bar{\theta}) d\bar{x} d\cos\bar{\theta}, \\ \nu_\mu: d\Gamma &= \frac{m_\mu^5 G^5}{32\pi^3} \left[\frac{\bar{x}^2(3-2\bar{x})}{6} \right. \\ &\quad \left. + \frac{\bar{x}^2(1-2\bar{x})}{6} \cos\bar{\theta} \right] d\bar{x} d\cos\bar{\theta}, \end{aligned} \quad (6)$$

where m_μ is the muon mass and G is the Fermi constant. Variables with a tilde represent the value in the muon rest frame. \bar{x} is $2\tilde{E}_\nu/m_\mu$, where \tilde{E}_ν is the neutrino energy and $\bar{\theta}$ the angle between the momentum of decay neutrino and the muon spin. The $\cos\bar{\theta}$ dependence in $d\Gamma$ represents the effect of muon polarization. Note that, for ν_e from the decay $\mu^+ \rightarrow e^+ + \nu_e + \bar{\nu}_\mu$, we should read

$\cos\bar{\theta}$ as $-\cos\bar{\theta}$ in Eq. (6). As mentioned before, μ^- from π^- decay is polarized to helicity $+$ by 30%, on the other hand, μ^+ from π^+ decay is polarized to the opposite direction; therefore, this effect is not canceled with $\bar{\nu}_e$ and ν_e .

In this calculation, we averaged these distributions over the angle between the momentum of the decay neutrino and the muon helicity after we transformed the distribution into the laboratory system.

B. Neutrino fluxes

Under these assumptions the solid-angle-averaged atmospheric neutrino fluxes at the earth's surface are represented by the following two equations. The ν_μ ($\bar{\nu}_\mu$) flux from the $\pi^\pm \rightarrow \mu^\pm + \nu_\mu$ ($\bar{\nu}_\mu$) process is

$$\frac{dF_\nu}{dE_\nu} = N \int d\Omega \int dh \int dE_\pi \int dy \frac{d\Gamma_\nu(E_\nu, E_\pi)}{dE_\nu} D_\pi(E_\pi) R_\pi(E_\pi, h, y) \frac{d^2 J_\pi(E_\pi, y)}{dE_\pi dy}, \quad (7)$$

and the $\bar{\nu}_\mu$ (ν_μ) or ν_e ($\bar{\nu}_e$) flux from the $\mu^\pm \rightarrow \nu_\mu(\bar{\nu}_\mu) + \nu_e(\bar{\nu}_e) + e^\pm$ process is

$$\begin{aligned} \frac{dF_\nu}{dE_\nu} &= N \int d\Omega \int dz \int dE_\mu \int dh \int dE_\pi \int dy \left[\frac{d\Gamma_\nu^+(E_\nu, E_\mu)}{dE_\nu} D_\mu(E_\mu) R_\mu(E_\mu, z, h) \frac{d\Gamma_\mu^+(E'_\mu, E_\pi)}{dE'_\mu} \right]_{E'_\mu = E_\mu + \Delta E_\mu(z, h)} \\ &\quad \left. + (+ \rightarrow -) \right] \\ &\quad \times D_\pi(E_\pi) R_\pi(E_\pi, h, y) \frac{d^2 J_\pi(E_\pi, y)}{dE_\pi dy}, \end{aligned} \quad (8)$$

where N is the normalization factor which is determined by comparing the calculated muon flux at the Earth's surface with a measured one as mentioned before. E_X is the energy of X particle in the laboratory system and z, h, y represents the altitude of the production point of the neutrino, muon, and pion, respectively. $d\Gamma_\nu(E_\nu, E_\pi)/dE_\nu$ is the neutrino production energy spectrum from a pion decay, $D_X(E_X)$ is the decay rate of the X particle, and $R_X(E_X, h_1, h_2)$ is the possibility that an X particle produced at the altitude h_2 survives at the altitude h_1 with energy E_X . $d^2 J_\pi(E_\pi, y)/dE_\pi dy$ is the pion-production energy spectrum at altitude y . This is defined as

$$\begin{aligned} &\frac{d^2 J_\pi(E_\pi, y)}{dE_\pi dy} \\ &\equiv \sigma_{\text{in}} N_A \rho(y) \int_{E_\pi}^\infty \frac{d\Gamma_\pi(E_\pi, E_P)}{dE_\pi} \frac{d^2 J_P(E_P, y)}{dE_P dy} dE_P, \end{aligned} \quad (9)$$

where $d^2 J_P(E_P, y)/dE_P dy$ is the energy spectrum of the primary proton at altitude y , $d\Gamma_\pi(E_\pi, E_P)/dE_\pi$ the pion-production energy spectrum which is given by Eq.

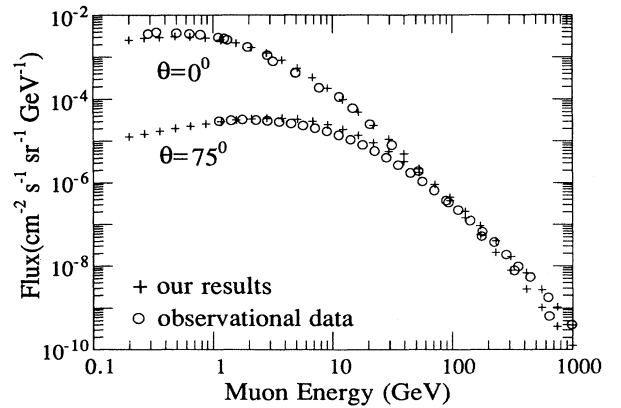


FIG. 1. Comparison between the results of our calculation with $p=1$ [see Eq. (5)] and the observational data (Refs. 14 and 16) of vertical (zenith angle is 0°) and horizontal (zenith angle is 75°) muon fluxes at the Earth's surface (magnetic latitude λ is 49.8°). Circle and cross represent the observational data and the results of our calculation, respectively. The shape of the calculated muon fluxes is in good agreement with the observational data for the vertical flux and both the shape and the absolute value fit the data for the horizontal one.

(5), σ_{in} the proton-proton inelastic cross section, and N_A the Avogadro number. $d\Gamma_{\nu}^{+,-}(E_{\nu}, E_{\mu})/dE_{\nu}$ are the neutrino-production energy spectra from helicity + and - muon decay, and $d\Gamma_{\mu}^{+,-}(E'_{\mu}, E_{\pi})/dE'_{\mu}$ are the helicity + and - muon-production energy spectra, respectively. $\Delta E_{\mu}(z, h)$ is the muon energy loss by ionizing the Earth's atmosphere. The muon energy at the altitude x satisfies the differential equation

$$\frac{dE_{\mu}(x)}{dx} = a\rho(x), \quad (10)$$

where a is the rate of ionization loss ($a = 2.06 \text{ MeV/g cm}^{-2}$) and $\rho(x)$ is the atmospheric density profile [see Eq. (4)], and

$$\begin{aligned} \Delta E_{\mu}(x_1, x_2) &\equiv E_{\mu}(x_2) - E_{\mu}(x_1) \\ &= a\rho_0 h_0 (e^{-x_1/h_0} - e^{-x_2/h_0}). \end{aligned} \quad (11)$$

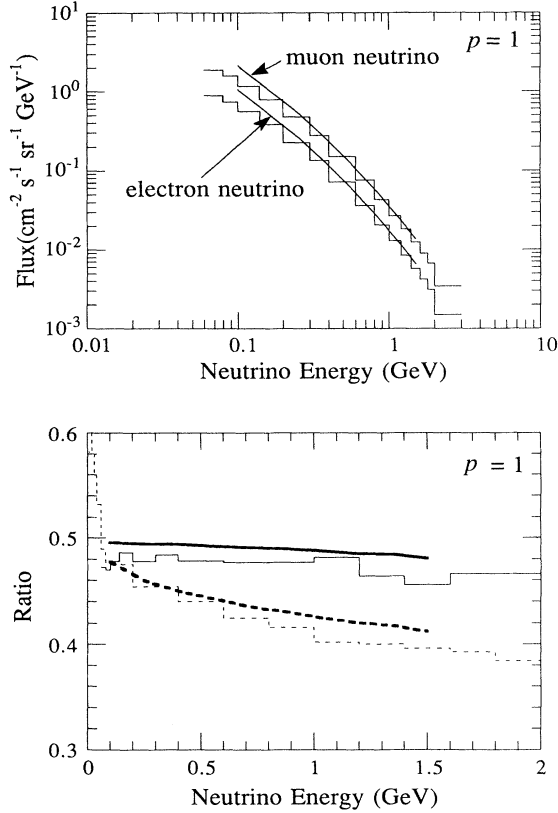


FIG. 2. Neutrino fluxes and the $(\nu_e + \bar{\nu}_e)/(\nu_{\mu} + \bar{\nu}_{\mu})$ ratio at the Kamioka site calculated with $p=1$ [see Eq. (5)]. The solid lines and the histograms show the results of our calculation and of Barr, Gaisser, and Stanev (Ref. 5), respectively. Although the calculated neutrino fluxes are larger than those of Barr, Gaisser, and Stanev by about 50% at 0.1 GeV of neutrino energy, the $(\nu_e + \bar{\nu}_e)/(\nu_{\mu} + \bar{\nu}_{\mu})$ ratio agrees within about 5% at all over the energy range for our calculation. The dashed line and the dashed histogram in the figure of $(\nu_e + \bar{\nu}_e)/(\nu_{\mu} + \bar{\nu}_{\mu})$ ratio shows the result of our calculation without muon polarization and of Gaisser, Stanev, and Barr (Ref. 2) which is also calculated without muon polarization, respectively.

III. RESULTS

We estimate Eqs. (7) and (8) by the numerical-integration program VEGAS. In order to check this calculation of atmospheric neutrino fluxes, we calculate the vertical and horizontal muon fluxes at the Earth's surface and compare them with the observational data^{14,16} (Fig. 1). As mentioned before, the normalization factor of neutrino fluxes is fixed by the vertical muon flux at the Earth's surface at the energy of 11.4 GeV. The shape of the calculated muon fluxes is in good agreement with the observational data for the vertical flux and both the shape and the absolute value fit the data for the horizontal one.

The calculated neutrino fluxes at the Kamioka site and the $(\nu_e + \bar{\nu}_e)/(\nu_{\mu} + \bar{\nu}_{\mu})$ ratio with the standard value of p ($=1$) [see Eq. (5)] are given in Fig. 2 with the results of Barr, Gaisser, and Stanev⁴ for comparison. Although the absolute values of the calculated neutrino fluxes are larger than those of Barr, Gaisser, and Stanev by about 50% at 0.1 GeV of neutrino energy, they are in good agreement above 0.2 GeV, and the $(\nu_e + \bar{\nu}_e)/(\nu_{\mu} + \bar{\nu}_{\mu})$ ratio agrees within about 5% at all over the energy range for this calculation.

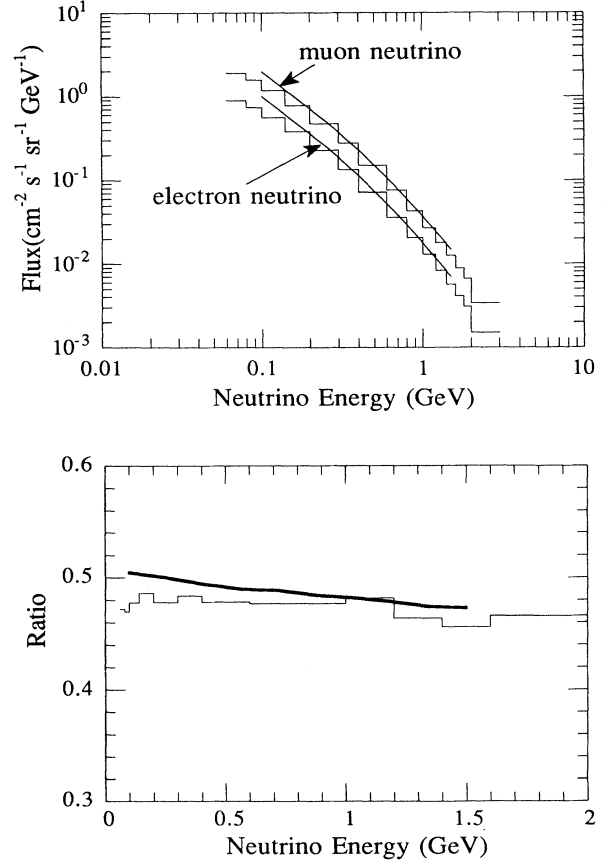


FIG. 3. Neutrino fluxes calculated by neglecting the primary protons with momentum smaller than the cutoff. Both the absolute value of the fluxes and the $(\nu_e + \bar{\nu}_e)/(\nu_{\mu} + \bar{\nu}_{\mu})$ ratio are in good agreement with those in Fig. 2. Therefore the effect of the secondary protons upon the atmospheric neutrino fluxes is negligible.

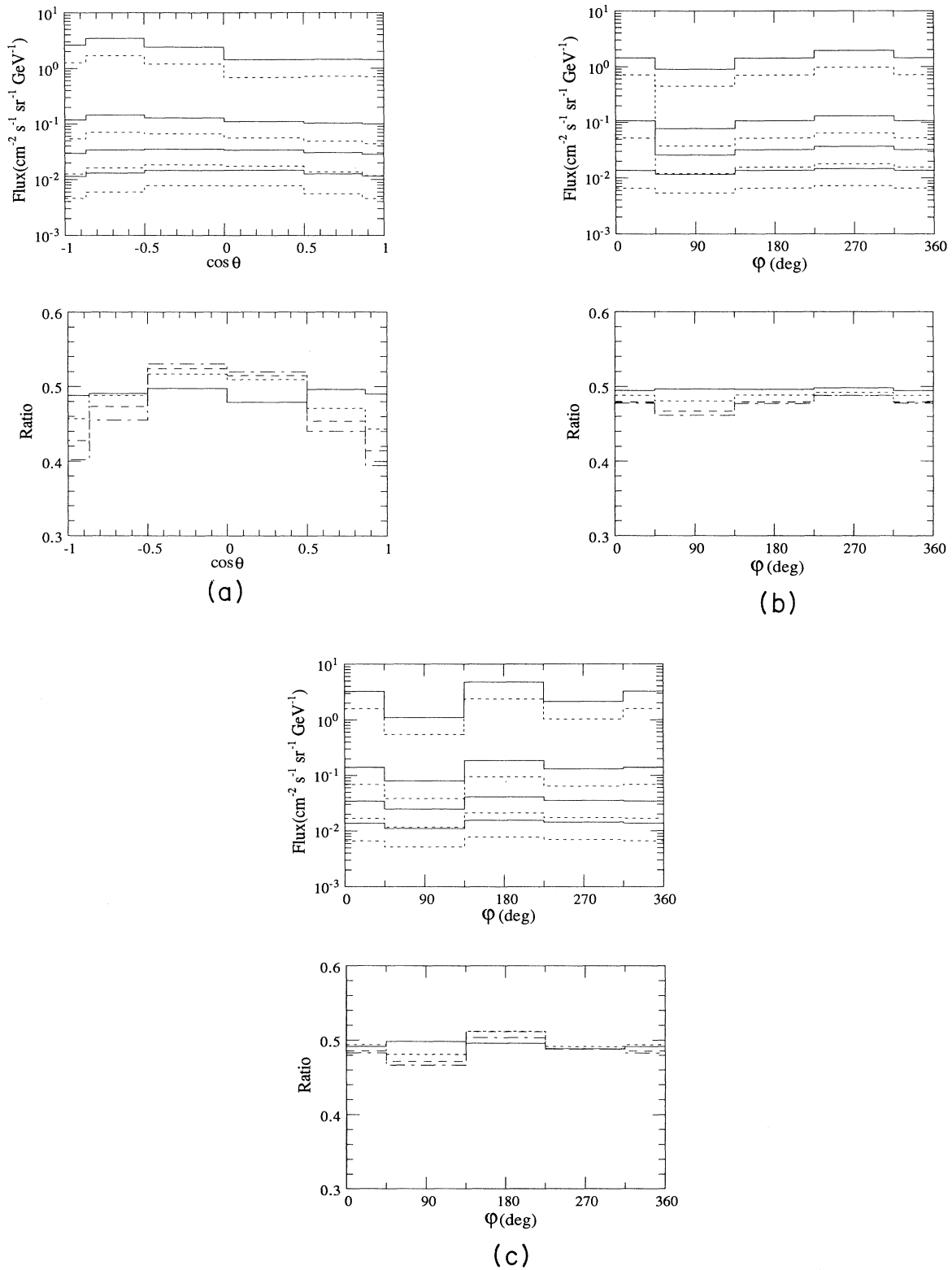


FIG. 4. (a) The zenith-angle distribution of neutrino fluxes and $(\nu_e + \bar{\nu}_e)/(\nu_\mu + \bar{\nu}_\mu)$ ratio where $\cos\theta=1$ corresponds to vertically downgoing neutrinos. (b) The azimuthal angle distribution for the downgoing neutrino. (c) The azimuthal angle distribution for the upgoing neutrino. The azimuthal angle is measured anticlockwise from magnetic south. In figures of flux, the solid line and the dashed line correspond to muon-neutrino flux and electron-neutrino flux, respectively, and the energy of neutrino is 0.1, 0.6, 1, and 1.5 GeV from top to bottom, respectively. In the figures of $(\nu_e + \bar{\nu}_e)/(\nu_\mu + \bar{\nu}_\mu)$ ratio, the solid line, dotted line, dashed line and dotted-dashed line correspond to the neutrino energy of 0.1, 0.6, 1, and 1.5 GeV, respectively.

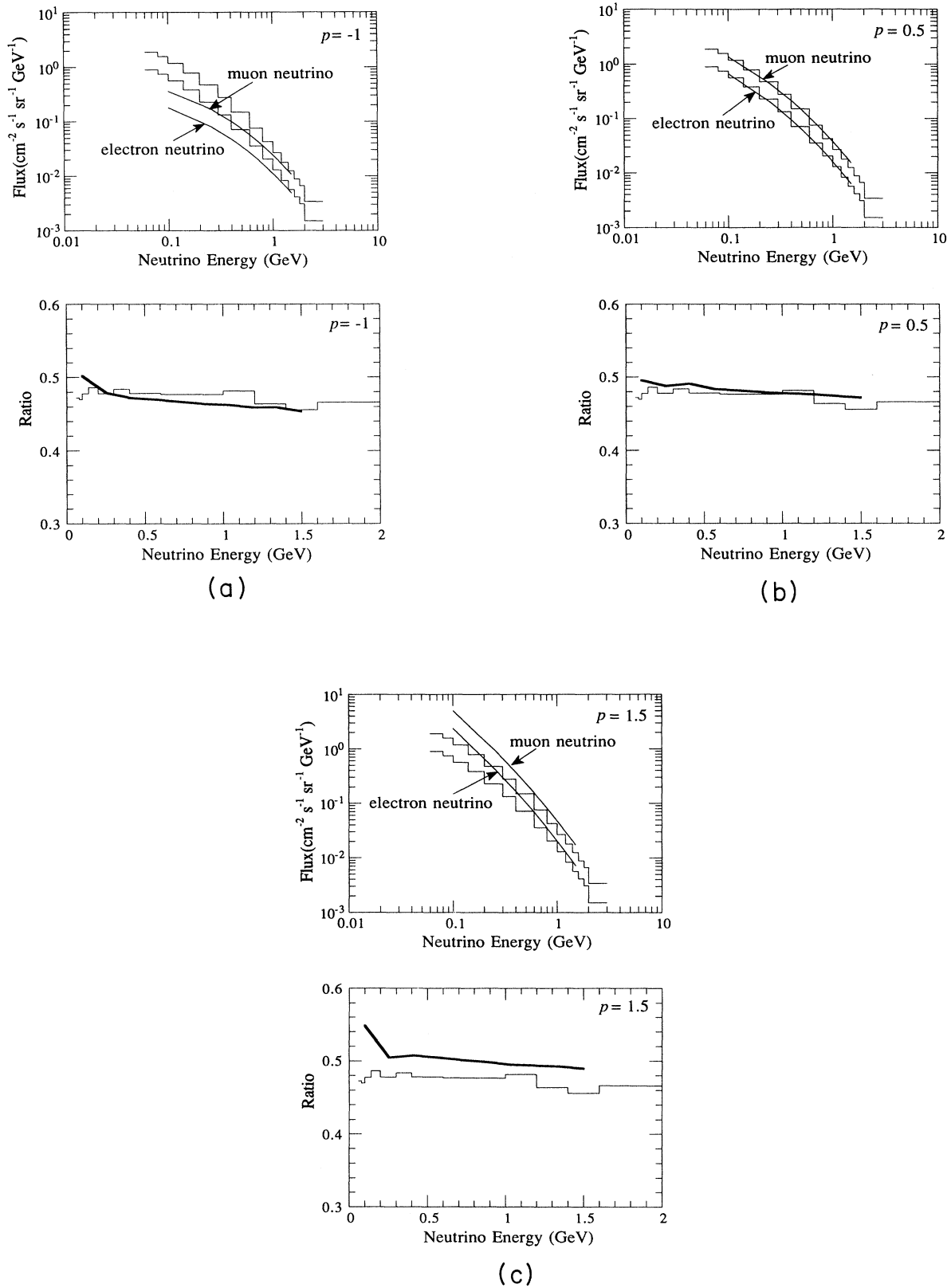


FIG. 5. Calculated neutrino fluxes and the $(\nu_e + \bar{\nu}_e)/(\nu_\mu + \bar{\nu}_\mu)$ ratio with some different values of p [see Eq. (5)]: (a) $p = -1$, (b) $p = 0.5$, (c) $p = 1.5$. The $(\nu_e + \bar{\nu}_e)/(\nu_\mu + \bar{\nu}_\mu)$ ratio for the different values of p are in good agreement with each other within at most 10%.

In Fig. 2, we also show the $(\nu_e + \bar{\nu}_e)/(\nu_\mu + \bar{\nu}_\mu)$ ratio without muon polarization. As mentioned before, the $(\nu_e + \bar{\nu}_e)/(\nu_\mu + \bar{\nu}_\mu)$ ratio with muon polarization is indeed larger than that without muon polarization (see Sec. II A 7, *Muon polarization*).

We show in Fig. 3 the results of calculation by neglecting the primary protons below the cutoff momentum. Both the absolute value of the fluxes and the $(\nu_e + \bar{\nu}_e)/(\nu_\mu + \bar{\nu}_\mu)$ ratio are in good agreement with those with the flat spectrum below the cutoff. Therefore the effect of the secondary protons upon the atmospheric neutrino fluxes is negligible in this calculation.

Figure 4 shows the angular distributions where θ is the zenith angle and φ is the azimuthal angle measured anticlockwise from magnetic South. The upgoing neutrino fluxes are larger than the downgoing ones at the low-energy region, because the geomagnetic cutoff for upgoing initial protons is effectively smaller than that for downgoing ones. The azimuthal angle distribution of the

downgoing neutrino fluxes is understood from the similar reason, i.e., for the same zenith angle θ , the smaller is $\sin\varphi$, the smaller is the geomagnetic cutoff [see Eq. (3)]. On the other hand, the azimuthal angle distribution of the upgoing neutrino fluxes is complicated but it can be understood in the same way.

The $(\nu_e + \bar{\nu}_e)/(\nu_\mu + \bar{\nu}_\mu)$ ratios of the vertically upgoing and vertically downgoing neutrinos are smaller than those of horizontally coming ones at the high-energy region. This is because some of the vertically coming muons with high energy reach the Earth's surface before they decay. Since the electron neutrinos are produced from only muon decays, the $(\nu_e + \bar{\nu}_e)/(\nu_\mu + \bar{\nu}_\mu)$ ratio of the vertically coming neutrinos becomes smaller than that of the horizontally coming ones.

The azimuthal angle distribution of the $(\nu_e + \bar{\nu}_e)/(\nu_\mu + \bar{\nu}_\mu)$ ratio is almost isotropic within 10%.

As mentioned before, since the value of p in the pion-production momentum spectrum is not well known, we

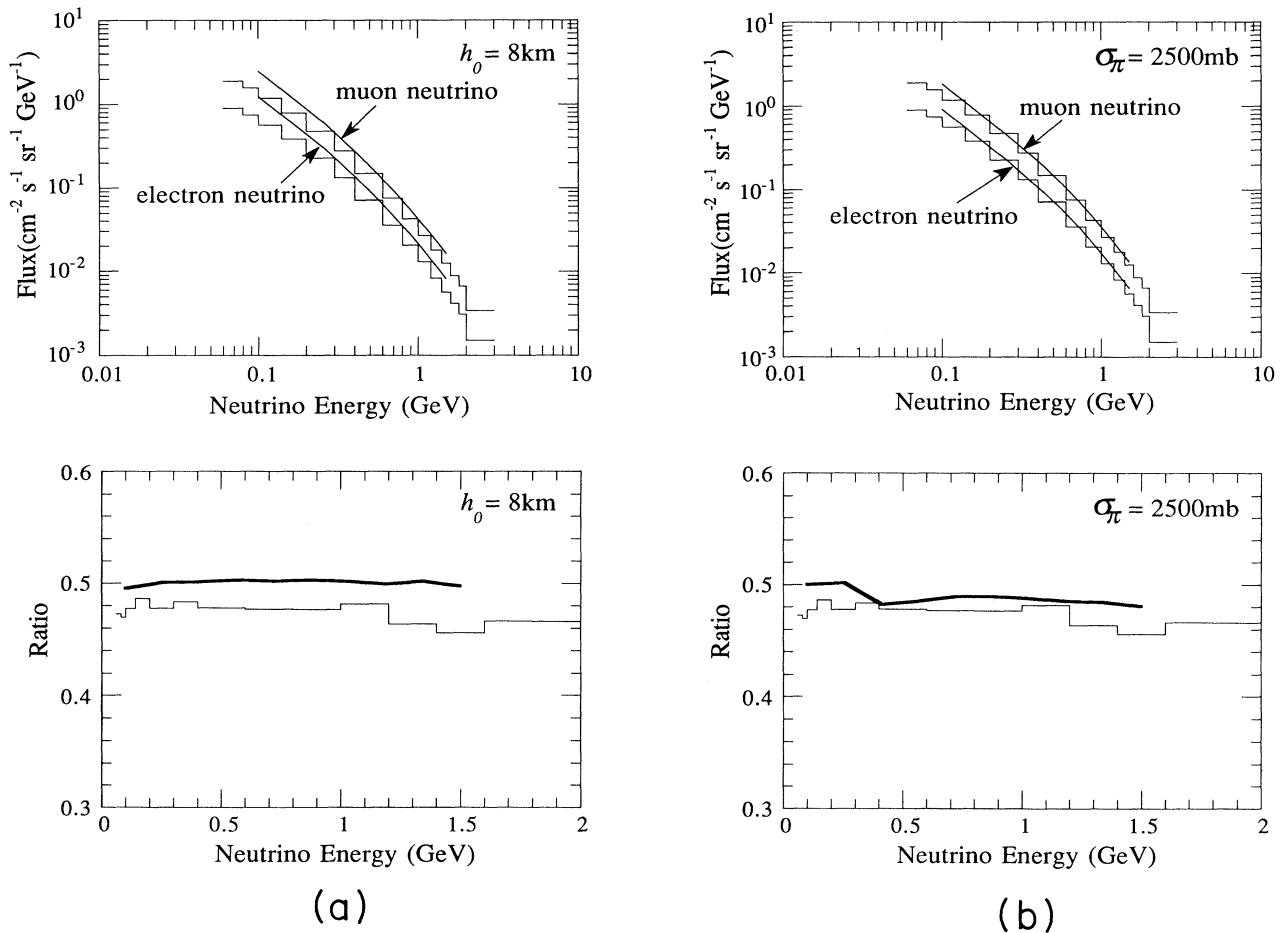


FIG. 6. Calculated neutrino fluxes and the $(\nu_e + \bar{\nu}_e)/(\nu_\mu + \bar{\nu}_\mu)$ ratio with (a) $h_0 = 8$ km which is the scale parameter of the atmospheric density profile (normal value is 6.42 km) and with (b) $\sigma_\pi = 2500$ mb which is the scattering cross section between pions and air nuclei at the low-energy region (normal value is 25 mb). Although the absolute value of resultant neutrino fluxes changes about 10%–20% from that in Fig. 2, the $(\nu_e + \bar{\nu}_e)/(\nu_\mu + \bar{\nu}_\mu)$ ratio is in good agreement within, at most, 4%.

calculate muon fluxes and neutrino fluxes with some different values of p [see Eq. (5)]. The effect of the difference of p upon the calculated muon fluxes is found to be negligible.

Figure 5 shows the calculated neutrino fluxes and the $(\nu_e + \bar{\nu}_e)/(\nu_\mu + \bar{\nu}_\mu)$ ratio with three different values of p . For example, the magnitude of neutrino fluxes with $p = 1.5$ is nearly fifteen times larger than that with $p = -1$ at 0.1 GeV of neutrino energy. This is because, for large p , pions from the scatterings between the initial protons and air nuclei tend to be produced with low energy; as a result, low-energy neutrinos increase. However, the $(\nu_e + \bar{\nu}_e)/(\nu_\mu + \bar{\nu}_\mu)$ ratios for the different values of p are in good agreement with each other within, at most, 10%.

Let us consider the $\bar{\nu}_e/\nu_e$ ratio. The source of $\nu_e(\bar{\nu}_e)$ is $\mu^+(\mu^-)$ from $\pi^+(\pi^-)$ decay, but in this calculation we do not distinguish $\mu^-(\pi^-)$ from $\mu^+(\pi^+)$. Therefore the $\bar{\nu}_e/\nu_e$ ratio cannot be determined in our scheme. However, we could estimate it by using experimental data. Since the source of $\nu_e(\bar{\nu}_e)$ is $\mu^+(\mu^-)$, the $\bar{\nu}_e/\nu_e$ ratio is expected to be roughly the same as the μ^-/μ^+ ratio at the Earth's surface. The observational value of the μ^-/μ^+ ratio is 0.77–0.83 at the muon energy between 3 GeV and 10 TeV.¹⁷ Although the energy range of these experimental data is higher than that of muons which produce the neutrinos with energy between 0.1 and 1.5 GeV, the experimental data show no clear dependence on muon energy. Hence the μ^-/μ^+ ratio or the $\bar{\nu}_e/\nu_e$ ratio is expected to be about 0.8 at the lower-energy region. Therefore this effect on the observed events of Kamiokande II may be small.

At last we mention the dependence of the resultant neutrino fluxes on other parameters. We calculate the neutrino fluxes changing the scale parameter or the scattering cross section between pions and air nuclei at the low-energy region within the range where they do not change the calculated muon fluxes at the Earth's surface. For example, we take 8 km for the scale parameter of atmosphere (the standard value is 6.42 km) and 2500 mb for the scattering cross section below 1 GeV of pion

momentum (the standard value is 25 mb) (Fig. 6). Although the absolute values of the resultant neutrino fluxes change about 10%–20%, the $(\nu_e + \bar{\nu}_e)/(\nu_\mu + \bar{\nu}_\mu)$ ratios agree with that of the standard value within, at most, 4% (see Fig. 2).

IV. CONCLUSION

We calculate the atmospheric neutrino fluxes semi-analytically. In summary, the resultant neutrino fluxes agree with those of the previous works.^{2,4} In particular, the $(\nu_e + \bar{\nu}_e)/(\nu_\mu + \bar{\nu}_\mu)$ ratio is in good agreement.

Furthermore, we calculate them with changing the value of some parameters as far as unphysical region, in order to estimate the influence of these parameters upon the fluxes and the $(\nu_e + \bar{\nu}_e)/(\nu_\mu + \bar{\nu}_\mu)$ ratio. As a result, it is found that the $(\nu_e + \bar{\nu}_e)/(\nu_\mu + \bar{\nu}_\mu)$ ratio is almost independent of the value of p in the pion-production momentum spectrum, the scale parameter of atmosphere, and the scattering cross section between pions and air nuclei at the low-energy region. Therefore we expect that the $(\nu_e + \bar{\nu}_e)/(\nu_\mu + \bar{\nu}_\mu)$ ratio is almost independent of the way and/or the details of calculation and it is very difficult to explain the data from Kamiokande II within the frame of the standard model. In other words, if we take the observational data seriously, it suggests the existence of new phenomena such as neutrino oscillations.

ACKNOWLEDGMENTS

We are grateful to T. Yanagida and M. Yoshimura for helpful discussions and to F. Takagi for useful comments on hadron physics. The numerical computations were carried out on the ACOS S-2000 at the Bubble Chamber Physics Laboratory of Tohoku University and on the FACOM M780 at the Astronomical Data Analysis Center of National Astronomical Observatory of Japan. This research was supported in part by the Japanese Grant in Aid for Science Research Fund of the Ministry of Education, Science and Culture Grants No. 02640213 and No. 02211201.

¹K. S. Hirata *et al.*, Phys. Lett. B **205**, 416 (1988).

²T. K. Gaisser, T. Stanev, and G. Barr, Phys. Rev. D **38**, 85 (1988).

³Y. Totsuka, in *Last Workshop on Grand Unification*, proceedings, Chapel Hill, North Carolina, 1989, edited by P. H. Frampton (World Scientific, Singapore, 1989), p. 3.

⁴G. Barr, T. K. Gaisser, and T. Stanev, Phys. Rev. D **39**, 3532 (1989).

⁵W. Gajewski, in *Proceedings of the 24th International Conference on High Energy Physics*, Munich, West Germany, 1988, edited by R. Kotthaus and J. H. Kuhn (Springer, Berlin, 1988).

⁶Ch. Berger *et al.*, Phys. Lett. B **227**, 489 (1989).

⁷S. Ragazzi, in *Tests of Fundamental Laws in Physics*, proceedings of the 24th Rencontre de Moriond, Les Arcs, France, 1989, edited by O. Fackler and J. Tran Thanh Van (Editions

Frontières, Gif-sur-Yvette, 1989).

⁸J. G. Learned, S. Pakvasa, and T. J. Weiler, Phys. Lett. B **207**, 79 (1988); K. Hidaka, M. Honda, and S. Midorikawa, Phys. Rev. Lett. **61**, 1537 (1988); V. Barger and K. Whisnant, Phys. Lett. B **209**, 365 (1988); M. Takita, Ph.D. thesis, University of Tokyo, 1989.

⁹E. V. Bugaev and V. A. Naumov, Phys. Lett. B **232**, 391 (1989); M. Honda, K. Kasahara, K. Hidaka, and S. Midorikawa, *ibid.* **248**, 193 (1990).

¹⁰E.g., see J. A. Simpson, Annu. Rev. Nucl. Part. Sci. **33**, 323 (1983).

¹¹C. Störmer, Astrophys. J. **1**, 237 (1930); D. J. Cooke, Phys. Rev. Lett. **51**, 320 (1983).

¹²H. Lee and S. A. Bludman, Phys. Rev. D **37**, 122 (1988).

¹³E.g., see T. Eichten *et al.*, Nucl. Phys. **B44**, 333 (1972).

¹⁴O. C. Allkofer, K. Carstensen, and W. D. Dau, Phys. Lett.

- 36B**, 425 (1971).
- ¹⁵L. V. Volkova, in *Cosmic Gamma Rays, Neutrinos and Related Astrophysics*, edited by M. M. Shapiro and J. P. Wefel (Kluwer Academic, Dordrecht, 1988), p. 139; S. Barr, T. K. Gaisser, P. Lipari, and S. Tilav, *Phys. Lett. B* **214**, 147 (1988).
- ¹⁶H. Jokisch *et al.*, *Phys. Rev. D* **19**, 1368 (1979).
- ¹⁷Y. Muraki *et al.*, *Phys. Rev. D* **28**, 40 (1983); O. C. Allkofer *et al.*, *Phys. Rev. Lett.* **41**, 832 (1978); G. D. Badhwar, S. A. Stephens, and R. L. Golden, *Phys. Rev. D* **15**, 820 (1977), and references therein.